

## **Cation vacancy activating surface neighboring sites for efficient CO<sub>2</sub> photoreduction on Bi<sub>4</sub>Ti<sub>3</sub>O<sub>12</sub> nanosheets**

Lizhen Liu<sup>a</sup>, Jingcong Hu<sup>b</sup>, Ben Lei<sup>c</sup>, Hongwei Huang<sup>a,\*</sup> and Yue Lu<sup>b,\*</sup>

<sup>a</sup>Beijing Key Laboratory of Materials Utilization of Nonmetallic Minerals and Solid Wastes, School of Materials Science and Technology, China University of Geosciences, Beijing 100083, P. R. China

E-mail: [hwh@cugb.edu.cn](mailto:hwh@cugb.edu.cn)

<sup>b</sup>Beijing Key Laboratory of Microstructure and Properties of Solids, Faculty of Materials and Manufacturing, Beijing University of Technology, Beijing 100124, P. R. China.

E-mail: [luyue@bjut.edu.cn](mailto:luyue@bjut.edu.cn)

<sup>c</sup>Research Center for Environmental and Energy Catalysis, Institute of Fundamental and Frontier Sciences, University of Electronic Science and Technology of China, Chengdu 611731, P. R. China.

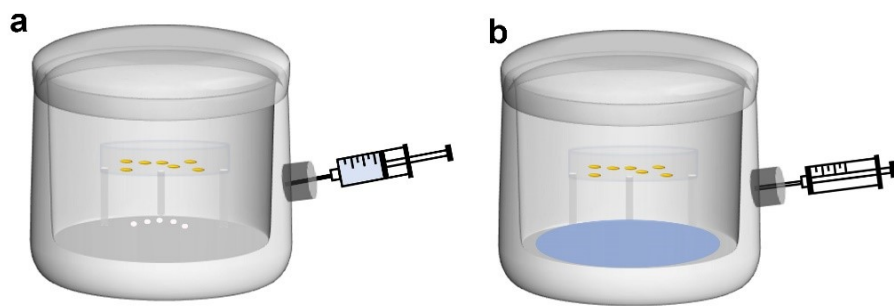


**Figure S1.** Schematic illustration of CO<sub>2</sub> photoreduction reactor.

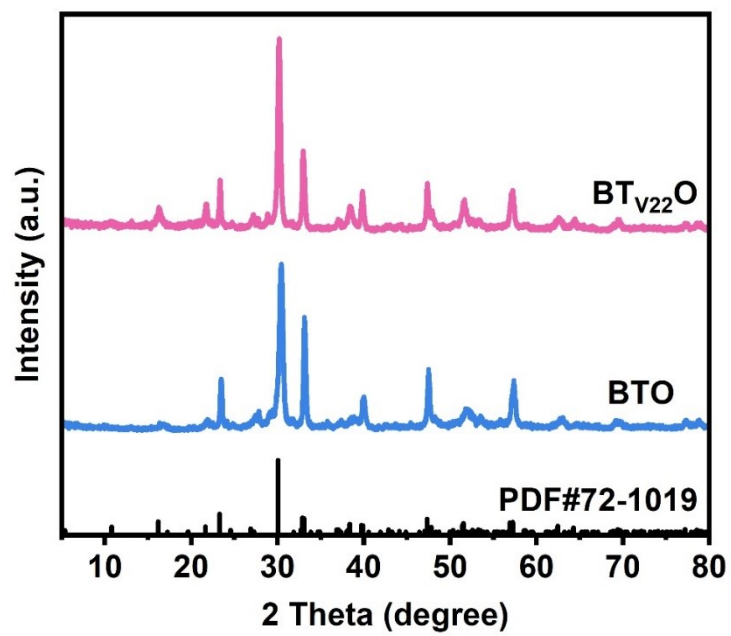


**Figure S2.** XRD patterns of BTO and  $BT_{V22}O$ .

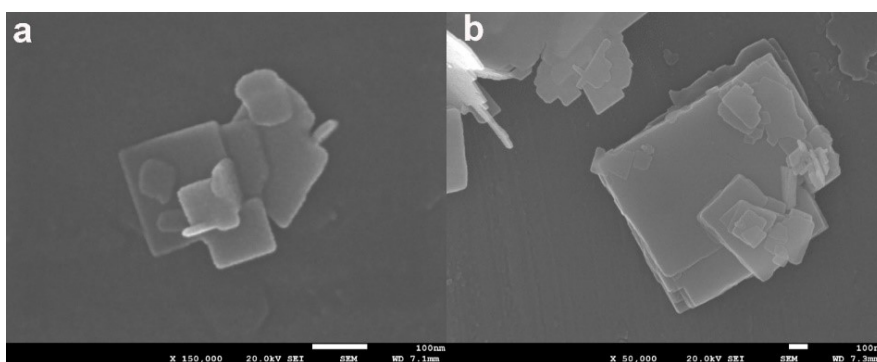


**Figure S3.** SEM images of (a) BTO and (b) BT<sub>V22</sub>O.

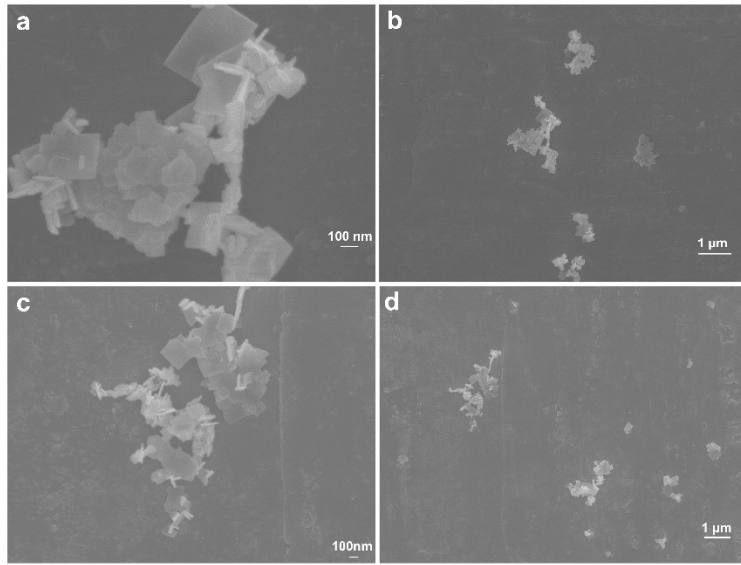


**Figure S4.** SEM images with different magnifications of (a, b) BTO and (c, d) BT<sub>V22</sub>O.

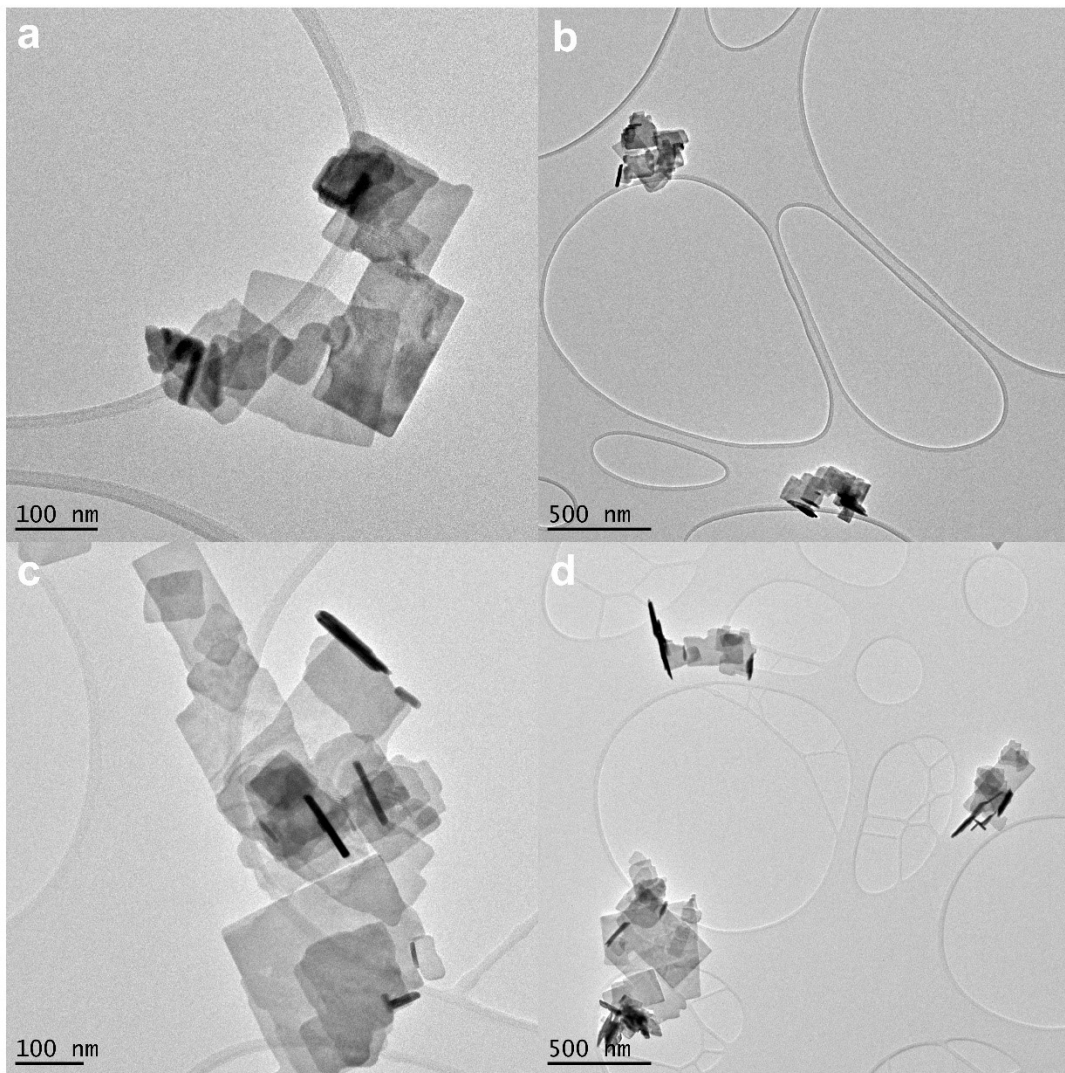


**Figure S5.** TEM images with different magnifications of (a, b) BTO and (c, d)  $\text{BT}_{\text{V}22}\text{O}$ .

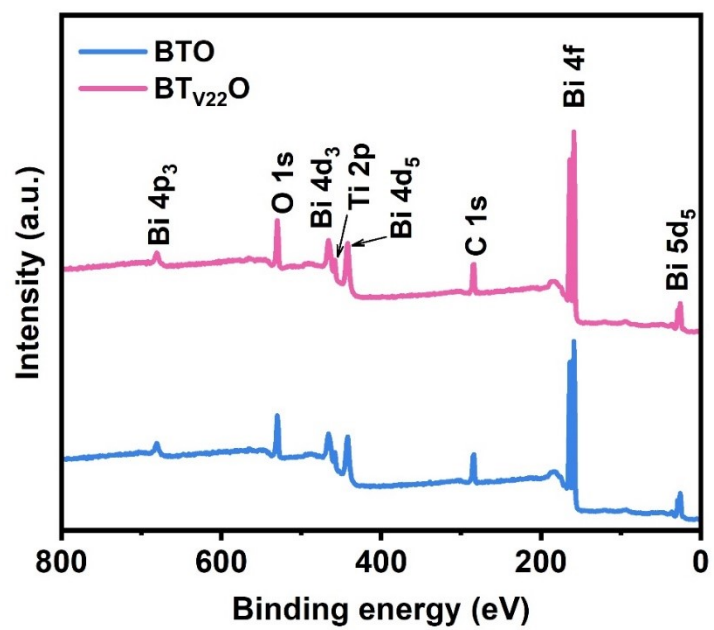
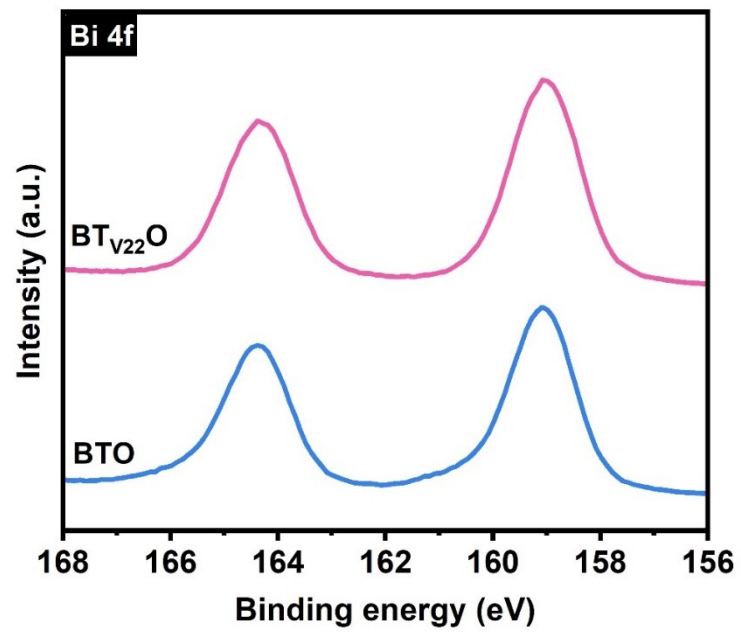
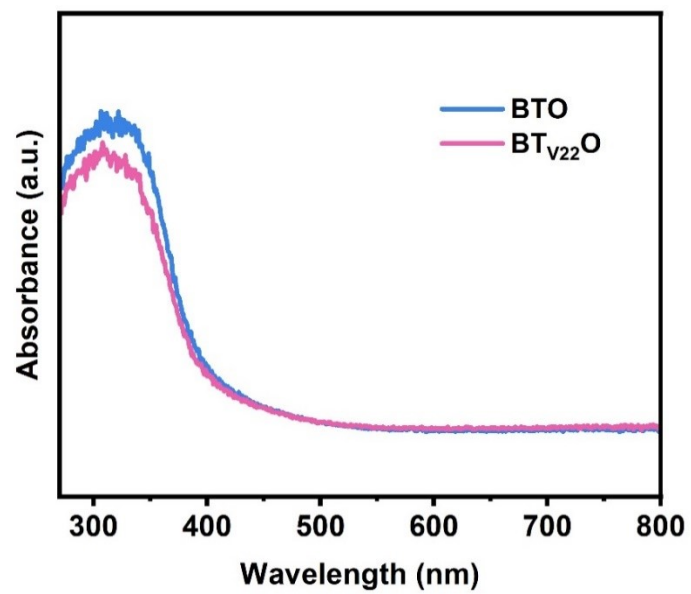


Figure S6. XPS spectra of BTO and  $\text{BT}_{\text{V}22}\text{O}$ .



**Figure S7.** XPS spectra of Bi 4f of BTO and  $BT_{V22}O$ .





**Figure S8.** DRS spectra of BTO and  $BT_{V22}O$ .

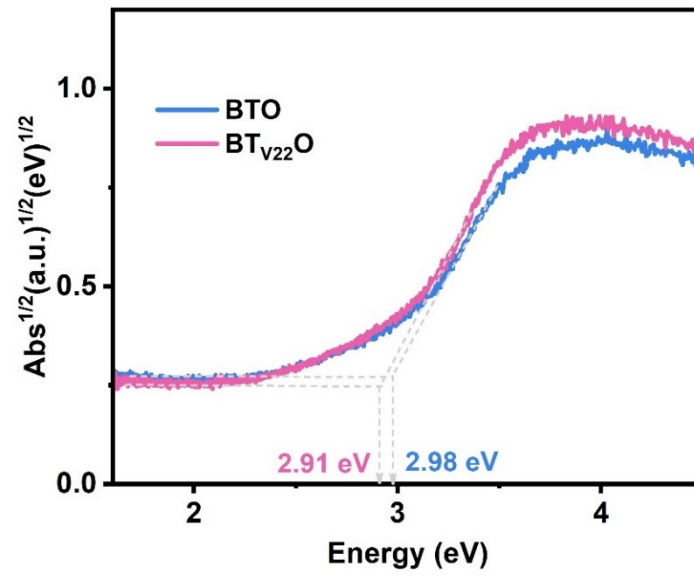


**Figure S9.** Bandgap of BTO and  $\text{BT}_{\text{V}22}\text{O}$ .

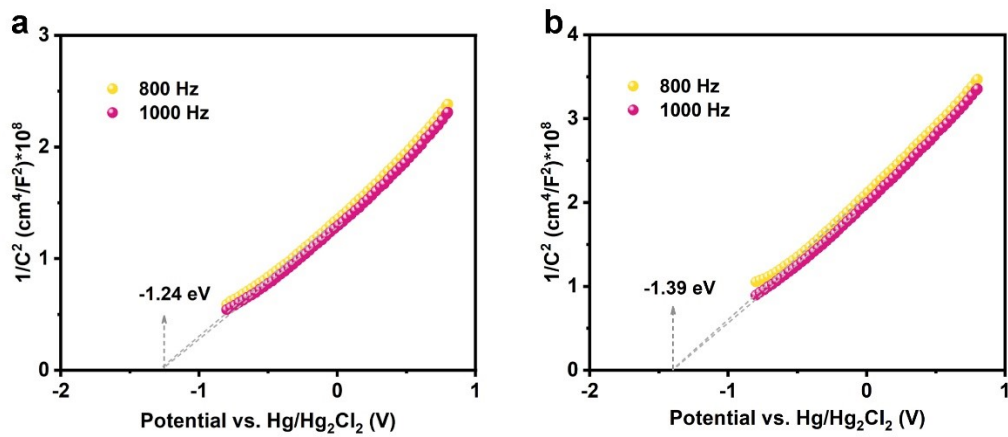


**Figure S10.** Mott-Schottky plots of (a) BTO and (b) BT<sub>V22</sub>O.

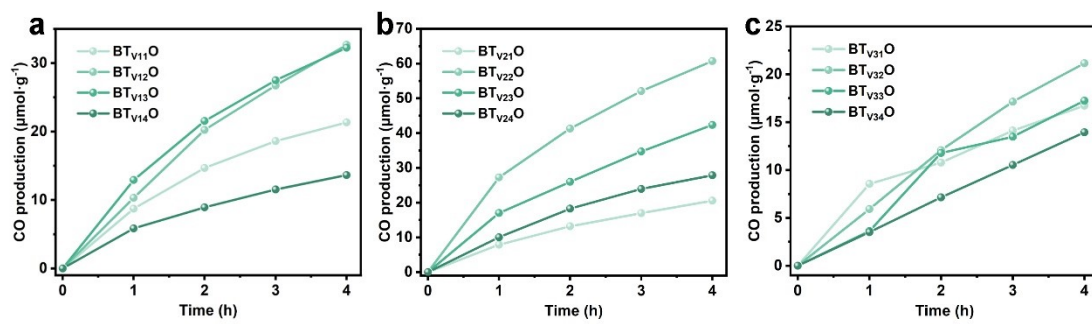


**Figure S11.** (a-c) Time-dependence CO production of BT<sub>VXY</sub>O (X=1, 2, 3; Y=1, 2, 3, 4).

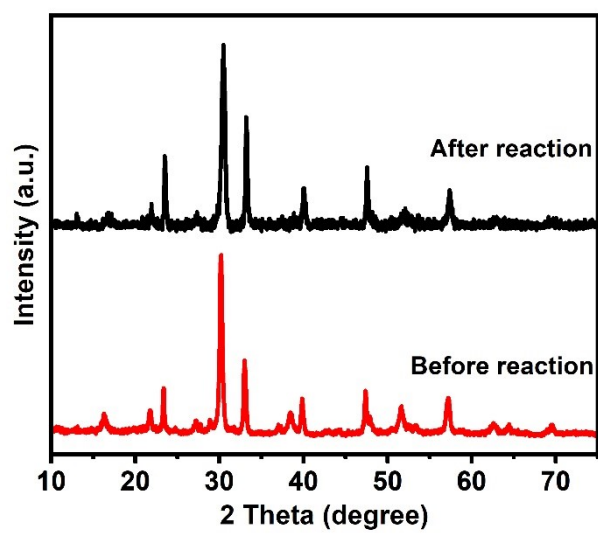


**Figure S12.** XRD patterns of  $\text{BT}_{V22}\text{O}$  before and after photoreduction reaction.

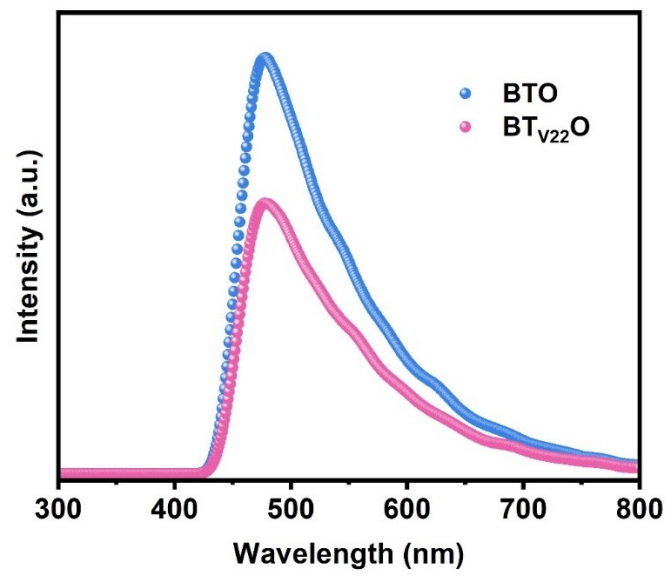


**Figure S13.** PL spectra of BTO and  $\text{BT}_{V22}\text{O}$ .

**Table S1.** The concentrations (wt%) of Ti vacancy. (0.1, 0.5 and 1 M corresponding to the NaOH concentrations; 15, 30, 60 and 90 min corresponding to the treating time)

Treating time	0.1 M	0.5 M	1.0 M
15 min	1.08	1.82	3.47
30 min	4.38	7.20	10.01
60 min	4.63	9.84	10.34
90 min	10.01	15.55	15.88

**Table S2.** Comparison of the CO<sub>2</sub> photoreduction activity of BTO with the some selected Bi-based catalysts reported in the references.

<b>Photocatalyst</b>	<b>Light sources</b>	<b>Photoactivity</b>	<b>Ref.</b>
BT <sub>V22</sub> O	300W Xe lamp	CO: 15.17 μmol g <sup>-1</sup> h <sup>-1</sup>	This work
Bi <sub>4</sub> Ti <sub>3</sub> O <sub>12</sub> hollow-spheres	300W Xe lamp	CO: 13.1 μmol g <sup>-1</sup> h <sup>-1</sup>	[1]
Bi <sub>2</sub> O <sub>2</sub> (OH)(NO <sub>3</sub> ) with Br grafting	300W Xe lamp	CO: 8.12 μmol g <sup>-1</sup> h <sup>-1</sup>	[2]
BiVO <sub>4</sub> /Bi <sub>4</sub> Ti <sub>3</sub> O <sub>12</sub> heterojunction	300W Xe lamp	CO: 13.29 μmol g <sup>-1</sup> h <sup>-1</sup>	[3]
Hollow-hierarchical Bi <sub>2</sub> WO <sub>6</sub> nanosheets	300 W Xe lamp	CH <sub>4</sub> : 2.6 μmol g <sup>-1</sup> h <sup>-1</sup>	[4]
Bi <sub>2</sub> MoO <sub>6</sub>	300W Xe lamp	CO: 14.38 μmol g <sup>-1</sup> h <sup>-1</sup>	[5]
BiOI flowerlike hierarchical structures	300W Xe lamp	CH <sub>4</sub> : 0.40 μmol g <sup>-1</sup> h <sup>-1</sup>	[6]
g-C <sub>3</sub> N <sub>4</sub> /BiOCl heterostructures with OVs	300W Xe lamp	CO: 4.73 μmol g <sup>-1</sup> h <sup>-1</sup>	[7]



## References

- [1] Y.Q. Wang, X.C. Zhang, C.M. Zhang, R. Li, Y.F. Wang, C.M. Fan, Novel Bi<sub>4</sub>Ti<sub>3</sub>O<sub>12</sub> hollow-spheres with highly-efficient CO<sub>2</sub> photoreduction activity, *Inorganic Chemistry Communications*, 116 (2020) 107931.
- [2] L. Hao, L. Kang, H.W. Huang, L.Q. Ye, K.L. Han, S.Q. Yang, H.J. Yu, M. Batmunkh, Y.H. Zhang, T.Y. Ma, Surface-halogenation-induced atomic-site activation and local charge separation for superb CO<sub>2</sub> photoreduction, *Advanced Materials*, 31 (2019) 1900546.
- [3] X.Y. Wang, Y.S. Wang, M.C. Gao, J.N. Shen, X.P. Pu, Z.Z. Zhang, H.X. Lin, X.X. Wang, BiVO<sub>4</sub>/Bi<sub>4</sub>Ti<sub>3</sub>O<sub>12</sub> heterojunction enabling efficient photocatalytic reduction of CO<sub>2</sub> with H<sub>2</sub>O to CH<sub>3</sub>OH and CO, *Applied Catalysis B-Environmental*, 270 (2020) 118876.
- [4] L.B. Xiao, R.B. Lin, J. Wang, C. Cui, J.Y. Wang, Z.Q. Li, A novel hollow-hierarchical structured Bi<sub>2</sub>WO<sub>6</sub> with enhanced photocatalytic activity for CO<sub>2</sub> photoreduction, *Journal of Colloid and Interface Science*, 523 (2018) 151-158.
- [5] S.G. Li, L.Q. Bai, N. Ji, S.X. Yu, S. Lin, N. Tian, H.W. Huang, Ferroelectric polarization and thin-layered structure synergistically promoting CO<sub>2</sub> photoreduction of Bi<sub>2</sub>MoO<sub>6</sub>, *Journal of Materials Chemistry A*, 8 (2020) 9268-9277.
- [6] G.J. Zhang, A.T. Su, J.W. Qu, Y. Xu, Synthesis of BiOI flowerlike hierarchical structures toward photocatalytic reduction of CO<sub>2</sub> to CH<sub>4</sub>, *Materials Research Bulletin*, 55 (2014) 43-47.
- [7] Y. Chen, F. Wang, Y.H. Cao, F.Y. Zhang, Y.Z. Zou, Z.A. Huang, L.Q. Ye, Y. Zhou, Interfacial oxygen vacancy engineered two-dimensional g-C<sub>3</sub>N<sub>4</sub>/BiOCl heterostructures with boosted photocatalytic conversion of CO<sub>2</sub>, *Acs Applied Energy Materials*, 3 (2020) 4610-4618.